Enhanced Exfoliation of Organoclay in Partially End-Functionalized Non-Polar Polymer

Xiaoliang Wang, Fangfang Tao, Gi Xue,* Jianjun Zhu, Tiehong Chen, Pingchuan Sun,* H. Henning Winter,* An-Chang Shi

We found that enhanced exfoliation of clay up to 20 wt.-% in non-polar polybutadiene (PB) if the PB was blended with a relatively small fraction of hydroxyl-terminated PB (HTPB). The choice of an intermediate polymer composition to enhance exfoliation was motivated by theoretical predictions of end-functionalizing effects of Balazs, Farmer, and coworkers. A combination of X-ray diffraction and rheological measurements were used to optimize HTPB content for enhanced exfoliation. We also observed the competition of the kinetic and thermodynamic processes during the ripening of the exfoliated clay structure.

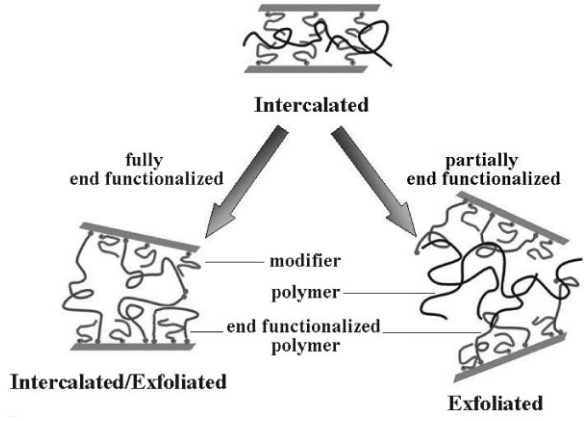

X. Wang, F. Tao, G. Xue
Department of Polymer Science and Engineering, Nanjing University, Nanjing 210093, P.R.China
J. Zhu, T. Chen, P. Sun
Key Laboratory of Functional Polymer Materials, Ministry of Education, College of Chemistry, Nankai University, Tianjin 300071, P.R.China
H. H. Winter
Department of Chemical Engineering and Department of Polymer Science and Engineering, University of Massachusetts, Amherst, Massachusetts 01003, USA
E-mail: winter@ecs.umass.edu
A.-C. Shi
Department of Physics and Astronomy, McMaster University, Hamilton, Ontario L8S 4M1, Canada

[a] Supporting information for this article is available at the bottom of the article's abstract page, which can be accessed from the journal's homepage at http://www.mme-journal.de, or from the author.

Introduction

Polymer–clay nanocomposites are known to acquire their advantageous physical properties when reaching a high degree of exfoliation and dispersion of the clay in the polymer matrix.[1–8] Fully exfoliated clay, however, is notoriously difficult to attain, particularly with non-polar polymers. Finding, understanding, and optimizing a simple and cost-effective method for preparing non-polar polymer–exfoliated-clay nanocomposites with high clay content remain significantly challenging.

Until now, only few approaches were effective in exfoliating clay in a non-polar polymer matrix. One such approach is in situ polymerization inside the gallery spaces of the clay.[3] Linear non-polar polymer–organoclay systems, such as PB/clay, can form intercalated structures (Figure. 1, top) but do not exfoliate by themselves.[9]

Macromol. Mater. Eng. 2009, 294, 190–195

DOI: 10.1002/mame.200800287

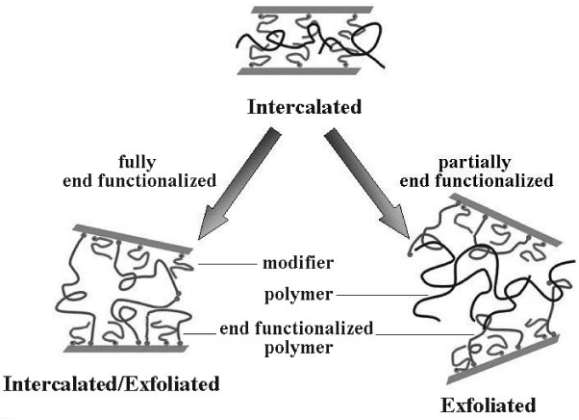

Figure 1. Schematic diagram related to the evolution of organoclay structures by blending end-functionalized polymer with non-polar polymer.

Exfoliation becomes possible through a strong interaction between the polymer chains and the clay surface. This interaction can be achieved by suitably end-functionalizing the polymer molecules[10–12] as demonstrated with maleic anhydride functionalized poly(propylene) (MA-PP),[6,7,13–15] and a new class of nanocomposites that utilize a dispersion of organoclay in end-functionalized, liquid polybutadiene (PB).[9,16–18] However, the clay loading at which the clay still exfoliated remained relatively low (typically less than 5 wt.-%).

For end-functionalized polymer–organoclay nanocomposites, the dispersion processes may cease at the intercalated structural state because of the gluing effect and/or the edge-blocking effect (as shown in Figure 1 left side). These phenomena were recently modeled by Balazs et al.[10] and Farmer et al.[19] Partially end-functionalizing of chains (instead of end-functionalizing all molecules in the polymer matrix) might thermodynamically favor the exfoliation process since gluing and edge-blocking are reduced. Based on these theoretical predictions, we started to partially end-functionalize the matrix polymer as a new experimental strategy for attempting clay exfoliation at high clay content, see Figure 1 (right side).

This model polymer study has the objectives (i) of finding out whether partial end-functionalizing of the matrix polymer is indeed preferable for preparing nanocomposites and, if yes, (ii) of optimizing HTPB content for achieving high clay loading with exfoliation. Experiments were performed with nanocomposites that contain organoclay in a matrix polymer blend of end-functionalized (OH group) and non-functionalized PB. Using a combination of rheology and X-ray, we observed the competition of the kinetic and thermodynamic processes during the ripening of the exfoliating clay structure.

Experimental Part

Material

A liquid hydroxyl-terminated 1,4-PB oligomer (HTPB) (Qilu Ethylene Chemical and Engineering Co. Ltd., China) serves as end-functionalized polymer. Two samples with molecular weights $\overline{M}_n = 2\,200$ and 4 200, (denoted as HTPB2200 and HTPB4200), with a polydispersity index of 2.6 were available. A liquid 1,2-PB oligomer of average molecular weight ($\overline{M}_n$) of 3300 (Aldrich Chemical Co.) without end groups was chosen as non-polar polymer. The microstructures of these polymers have been determined earlier by ^{1}H NMR (Varian UNITYplus-400 MHz NMR spectrometer).[9,16]

The organoclay (C18-clay) was prepared in small batches. A 10.0 g of industrially purified pristine montmorillonite (Tianjin Organic Clay Corp. China, cation exchange capacity is 1 mequiv $\cdot$ g^{-1}) was dispersed into 1 000 mL of distilled water at 87 °C for cation exchange with 3.5 g (equal to 1 mequiv $\cdot$ g^{-1}) of octadecyltrimethylammonium chloride (denoted as C18A) for 12 h. The processed clay was washed with distilled water and checked with a 0.1 N $AgNO_3$ solution for residual Cl^- ions. After the washing, the organoclay was dried at 87 °C for 12 h before use.

The C18A had been found to interact strongly with HTPB and poorly with PB.[9] Correspondingly, the modified clay interacts strongly with end-functionalized polymer and poorly with non-polar polymer.[10,17]

Desired amounts of organoclay were gently mixed into the PB/HTPB blends at room temperature as described previously.[9,16,17] The nanocomposite samples were then annealed under vacuum at 80 °C for a desired time. Here, we annealed at 80 °C because the temperature was high enough for the HTPB to penetrate the clay gallery and low enough to avoid oxidation. The HTPB fraction in the compatible polymer blend was varied at 0, 10, 25, 30, 40, 50, 75, 90, and 100 vol.-% in three series of samples (all the blends were transparent homogenous viscoelastic liquids at room temperature). Throughout the text, the sample names are abbreviated as BlendH4C15, BlendH4C20, and BlendH2C15, respectively, with the meaning of HTPB4200/PB blend with 15 and 20 wt.-% clay added, and a HTPB2200/PB blend with 15 wt.-% clay added.

X-Ray Diffraction

For determining the dispersion and exfoliation of the clay, X-ray diffraction (XRD) experiments were performed[1,20] in reflection mode in a Shimadzu XRD-6000 X-ray powder diffractometer with Cu Kα ($\lambda = 0.154$ nm) radiation at a generator voltage of 40 kV and a current of 100 mA.

Transmission Electron Microscopy (TEM)

Transmission electron microscopy is able to visualize the level of dispersion and homogeneity. TEM was carried out on a JEOL 2000FX electron microscope operated at 200 kV. Ultrathin sections (the edge of the epoxy embedded sample sheets) with a thickness of 100 nm were microtomed using a Sorvall Room Temperature Ultramicrotome.

Rheology Experiments

Rheology experiments were conducted in a stress-controlled rheometer (HAAKE RheoStress 600) with 35 mm diameter parallel

plate fixtures and a sample thickness of about 0.8 mm. Samples at 26 °C were sheared with a shear rate of 0.05 s^{-1} (rim shear rate). The shear rate was kept low to avoid orientation of polymer chains.[17] Freshly loaded samples were relaxed for 5 min before starting to shear. The time-resolved shear viscosity value was reported as function of aging time and HTPB fraction.

To compare the viscosity of different structural states, we used the relative viscosity instead of the absolute viscosity. For this purpose, a series of HTPB/PB blends were prepared without clay and their absolute viscosity was determined for future reference. The blend viscosity only weakly depends on the size of the HTPB fraction. With that, a relative viscosity was defined as ratio of the viscosities of the polymer mixed with clay and without clay.

Results

Rheology has been proven to be a powerful tool for studying polymer–clay interaction and polymer–clay orientation in nanocomposites.[1,14,17,21–24] The steady shear viscosity at low shear rates was found to be a sensitive indicator of the extent of polymer–clay interaction and dispersion. The effect of structure development at 80 °C was demonstrated on a freshly mixed nanocomposite which consisted of a blend of 26.5 vol.-% HTPB4200 and 73.5 vol.-% PB, and 15 wt.-% clay (abbreviated as BlendH4(26%)C15). The structure ripened quickly at 80 °C but changed very slowly at 26 °C. This slow-down at low temperature allowed us to "freeze" intermediate states of the structure ripening process and proceed with shear viscosity measurements at 26 °C. In this way, the evolving relative viscosity at 26 °C could serve as measure of structural evolution at 80 °C (Figure 2a). The shear viscosity is able to detect small differences in the dispersion of the clay.

The freshly mixed sample, before any annealing, already reached a relative viscosity of 15, i.e., its viscosity was 15 times the viscosity of the pure polymer without clay. In a first quick heating to 80 °C and instantaneous cooling back to 26 °C, the relative viscosity had jumped from 15 to 90 as marked in Figure 2a. The blend-character of the matrix polymer introduced novel characteristics in the ripening of the structure, especially at the late stages of ripening. During continued annealing at 80 °C, the relative viscosity grew rapidly at first, then reached a maximum after about 1 h, see Figure 2a, and decreased again when annealing for longer times. The rapid growth of the viscosity at early stages is attributed to a growing strong interaction between HTPB end-groups and the clay surface. The viscosity leveled off when the interaction of HTPB end-groups with the clays reached an optimum. Beyond that, more and more PB diffused into the clay galleries and diluted the strong interaction between HTPB and clay surfaces. Tie molecules between adjacent clay surfaces might have converted into loop molecules as described by

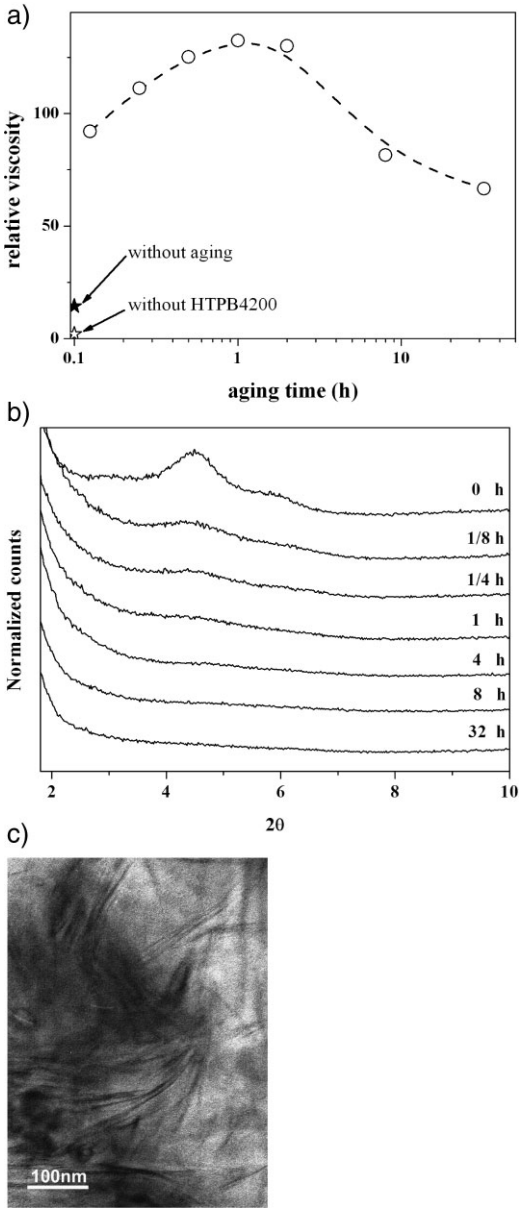

Figure 2. (a) The relative viscosity of BlendH4(26%)C15 as function of aging time at 80 °C. Empty and filled stars are the relative viscosities of PB–clay (15 wt.-%) and BlendH4(26%)C15 without aging, respectively. (b) Corresponding X-ray diffraction of BlendH4(26%)C15. (c) The TEM image of BlendH4(26%)C15 aging at 80 °C for 8 h, and the scale bar is 100 nm.

Malvaldi et al.[25]. This caused the viscosity decrease in the more exfoliated systems. The dilution effect can clearly be attributed to the non-functionalized PB since it only occurred when PB was in the sample.

The corresponding XRD pattern, Figure 2b, confirmed that the clay was only partially exfoliated at the first stage within 1 h, and that it exfoliated more thoroughly at increased aging times (causing the viscosity to decrease,

Macromol. Mater. Eng. **2009**, *294*, 190–195

Macromolecular Journals
DOI: 10.1002/mame.200800287

Figure 2a). The gallery distance between clay sheets became larger than 5 nm (no peaks appeared at 2θ lager than 1.7°) after 8 h. To explore this further, a BlendH4(26%)C15 sample, which had been annealed for 8 h at 80 °C, was imaged by TEM, (Figure 2c). Nearly all of the clay sheets were well exfoliated. Only a small fraction remained intercalated.

The HTPB/PB ratio was identified as one of the most influential parameters. To study its effect in more detail, we systematically changed the HTPB fraction while maintaining two other parameters constant: the clay content of 15 wt.-% and the sample annealing of 8 h at 80 °C (abbreviated as "BlendH4C15"). These conditions allowed sufficient time for the clay to acquire a stable time-independent state (denoted as "ripened" state in the following).

The XRD patterns of ripened nanocomposites at different HTPB4200 fractions, see Figure 3, start out with an intercalated clay structure in pure PB (0 vol.-% HTPB4200). Its pronounced peak at about 4.8° (2θ) is characteristic for intercalated clay. This peak weakened and shifted to smaller angles with increasing HTPB4200 content and vanished completely in the sample with 25 vol.-% HTPB4200, indicating complete exfoliation of the clay. When further increasing the fraction of HTPB4200 beyond 25 vol.-%, a broadened weak peak appeared at about 4.5° (2θ), indicating an intercalated/exfoliated clay structure. The same trends were observed in BlendH4C20 and BlendH2C15 samples and are not shown again (the optimal value were 35 and 10 vol.-%, respectively. See Supporting Information instead). This series of experiments indicates that the most favorable conditions for exfoliation are reached with intermediate HTPB4200 content.

The relative viscosity of ripened nanocomposites, Figure 4, also suggests that an intermediate HTPB concentration is optimum. The relative viscosity increases strongly when adding small amounts of HTPB. This is attributed to the strong HTPB–clay interaction, which leads to exfoliation in the ripened structure. The steep viscosity rise; however, ends at some sample-specific HTPB concentration beyond which the HTPB–clay interaction becomes less effective. A leveling-off concentration at this "turning point" can be defined as intercept of the initial and final slopes of the viscosity curves in Figure 4.

Discussion

Exfoliation in this study is envisioned as a two-step process in which the end-functionalized molecules enter the clay galleries first and widen the spacing between the clay sheets. This is followed by the diffusion of non-functionalized molecules into the widened galleries thereby increasing the spacing between clay sheets even further as required for exfoliation. Figure 1 schematically shows the evolution of clay structures in a blend–clay nanocomposite. The time evolution of structure gets expressed in the relative viscosity of Figure 2a.

The end-functionalized polymer is the minor component in the blend. Overly high concentrations of end-functionalized molecules would yield poor exfoliation since the telechelic chains would begin to bridge or glue adjacent clay sheets and prevent further chains from entering the galleries. Malvaldi et al.[25] has shown this as one of seven possible states of a telechelic polymer confined between two walls.

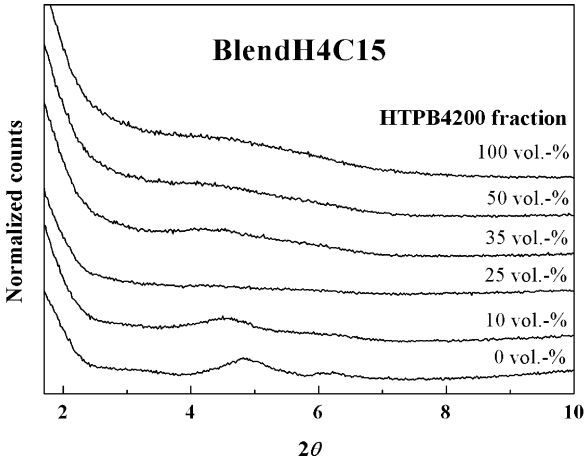

Figure 3. X-ray diffraction of BlendH4C15 nanocomposite gels with different HTPB4200 fractions, which had been annealed at 80 °C for 8 h.

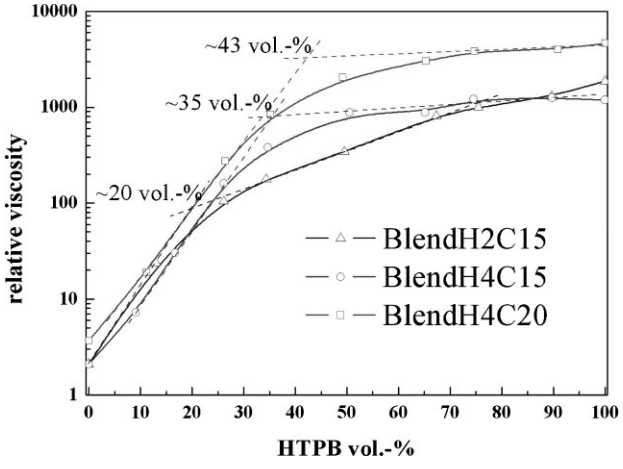

Figure 4. Relative shear viscosity at 26 °C after aging at 80 °C for 8 h as function of HTPB fraction for BlendH2C15, BlendH4C15, and BlendH4C20.

Optimum exfoliation conditions are expected to be reached at an intermediate HTPB/PB composition since the clay surface can only adsorb certain limited molar amounts of HTPB. The optimum conditions can be estimated from the location of the "turning points" in Figure 4: $2c_{HTPB}/M_{HTPB} = Ac_{clay}$, wherein the c_{HTPB} is the HTPB/PB fraction of the blend, M_{HTPB} is the molar weight of HTPB, c_{clay} is the clay content, and A is the assuming saturated adsorption amount per unit clay content. With the "turning point" as defined for Figure 4 data at 35 vol.-% HTPB4200 fraction for BlendH4C15 as a reference, one can roughly estimate optimal HTPB fraction for BlendH2C15 and BlendH4C20 to be 18 and 47 vol.-%, respectively. These calculated turning points are consistent with the results for different nanocomposites in Figure 4 (20 and 43 vol.-% HTPB content, respectively), which confirms our above assumption of surface saturation at intermediate HTPB fraction.

The optimal HTPB4200 fraction for BlendH4C15 nanocomposites with the highest degree of clay exfoliation was 25 vol.-% (as indicated in Figure 3), which is a little smaller than the turning point of the corresponding viscosity curve. The trend is the same for BlendH2C15 and BlendH4C20.

Molecular dynamics simulations of Farmer et al. [19] and SCFT studies of Balazs et al.[10,12] predict a large reduction of the free energy of the system in the presence of end-functionalized polymer. The intercalation process is kinetically controlled at early stages of a freshly mixed nanocomposite, and thermodynamics controls the later stages. The final exfoliated state is predicted to be thermodynamically favored. However, attaining this overall energy minimum requires long ripening times. Our experimental results are consistent with these theoretical predictions.

Conclusion

A compatible blend of end-functionalized PB with non-functionalized PB was found to effectively exfoliate organoclay in a clay–polymer nanocomposite. The PB/HTPB/clay system is suitable as model system for exploring the effects of partially end-functionalizing of non-polar polymers for nanocomposites. A small fraction of end-functionalized PB already has a large effect on internal structure. Three distinct phenomena could be identified: (i) increased network connectivity due to the presence of HTPB which resulted in a substantial viscosity increase in the ripened structure, (ii) sequential ripening processes in which HTPB molecules diffuse into the clay galleries first and PB molecules follow later, and (iii) the existence in an optimum PB/HTPB ratio for nanocomposites at high clay content. The existence of such optimum supports theoretical predictions of Balazs and Farmer.

The highest loading of exfoliated clay, as might be useful for preparing masterbatches for nanocomposites, was achieved with an intermediate fraction of end-functionalized PB as matrix polymer, much higher than with all end-functionalized or with all non-functionalized molecules. Rheology combined with XRD makes it possible to observe the structural evolution of clays from the aggregated state to exfoliation, and to estimate the optimal fraction of the end-functionalized polymer, especially for nanocomposites at high clay content.

Acknowledgements: We thank *Jintao Zhu* at UMass Amherst for his TEM-help. *The National Natural Science Foundation of China* (grants 50533020, 20825416, 20373029) and the State Scholarship Fund of China supported this study. H. H. W. acknowledges the support of *NSF-MRSEC* at UMass Amherst. A. C. S. acknowledges the support of the *Natural Science and Engineering Council (NSERC)* of Canada.

Received: September 22, 2008; Revised: December 3, 2008; Accepted: December 4, 2008; DOI: 10.1002/mame.200800287

Keywords: end-functionalized polymer; exfoliation; intercalation; nanocomposite; organoclay; rheology

[1] S. S. Ray, M. Okamoto, *Prog. Polym. Sci.* **2003**, *28*, 1539.
[2] T. J. Pinnavaia, G. W. Beale, "*Polymer-Clay Nanocomposites*", Wiley, New York 2000.
[3] W. R. Mariott, E. Y. X. Chen, *J. Am. Chem. Soc.* **2003**, *125*, 15726.
[4] D. R. Robello, N. Yamaguchi, T. Blanton, C. Barnes, *J. Am. Chem. Soc.* **2004**, *126*, 8118.
[5] K. Haraguchi, M. Ebato, T. Takehisa, *Adv. Mater.* **2006**, *18*, 2250.
[6] E. Manias, A. Touny, L. Wu, K. Strawhecker, B. Lu, T. C. Chung, *Chem. Mat.* **2001**, *13*, 3516.
[7] Z. M. Wang, H. Nakajima, E. Manias, T. C. Chung, *Macromolecules* **2003**, *36*, 8919.
[8] Y. Wang, Q. Zhang, Q. Fu, *Macromol. Rapid Commun.* **2003**, *24*, 231.
[9] T. H. Chen, J. J. Zhu, B. H. Li, S. Y. Guo, Z. Y. Yuan, P. C. Sun, D. T. Ding, A. C. Shi, *Macromolecules* **2005**, *38*, 4030.
[10] A. C. Balazs, C. Singh, E. Zhulina, *Macromolecules* **1998**, *31*, 8370.
[11] R. A. Vaia, E. P. Giannelis, *Macromolecules* **1997**, *30*, 7990.
[12] Y. Lyatskaya, A. C. Balazs, *Macromolecules* **1998**, *31*, 6676.
[13] M. J. Solomon, A. S. Almusallam, K. F. Seefeldt, A. Somwangthanaroj, P. Varadan, *Macromolecules* **2001**, *34*, 1864.
[14] K. Wang, Z. C. Hou, P. Zhao, J. Deng, Q. Zhang, Q. Fu, X. Dong, D. J. Wang, C. C. Han, *J. Chem. Phys.* **2007**, *127*, 7.
[15] Q. Zhang, Y. Wang, Q. Fu, *J. Polym. Sci. Pt. B-Polym. Phys.* **2003**, *41*, 1.

DOI: 10.1002/mame.200800287

[16] P. C. Sun, J. J. Zhu, T. H. Chen, Z. Y. Yuan, B. H. Li, Q. H. Jin, D. T. Ding, A. C. Shi, *Chin. Sci. Bull.* **2004**, *49*, 1664.
[17] X. L. Wang, Y. Gao, K. M. Mao, G. Xue, T. H. Chen, J. J. Zhu, B. H. Li, P. C. Sun, Q. H. Jin, D. T. Ding, A. C. Shi, *Macromolecules* **2006**, *39*, 6653.
[18] J. J. Zhu, X. L. Wang, F. F. Tao, G. Xue, T. H. Chen, P. C. Sun, Q. H. Jin, D. T. Ding, *Polymer* **2007**, *48*, 7590.
[19] A. Sinsawat, K. L. Anderson, R. A. Vaia, B. L. Farmer, *J. Polym. Sci. Pt. B-Polym. Phys.* **2003**, *41*, 3272.
[20] I. J. Chin, T. Thurn-Albrecht, H. C. Kim, T. P. Russell, J. Wang, *Polymer* **2001**, *42*, 5947.
[21] R. Krishnamoorti, K. Yurekli, *Curr. Opin. Colloid Interface Sci.* **2001**, *6*, 464.
[22] M. Y. Gelfer, C. Burger, B. Chu, B. S. Hsiao, A. D. Drozdov, M. Si, M. Rafailovich, B. B. Sauer, J. R. W. Gilman, *Macromolecules* **2005**, *38*, 3765.
[23] M. Y. Gelfer, H. H. Song, L. Z. Liu, B. S. Hsiao, B. Chu, M. Rafailovich, M. Y. Si, V. Zaitsev, *J. Polym. Sci. Pt. B-Polym. Phys.* **2003**, *41*, 44.
[24] P. Cassagnau, *Polymer* **2008**, *49*, 2183.
[25] M. Malvaldi, G. Allegra, F. Ciardelli, G. Raos, *J. Phys. Chem. B* **2005**, *109*, 18117.